

# Status of baryon femtoscopy at BM@N

L.Kovachev, A.Stavinskiy for BM@N collaboration

1. Femtoscopy method
2. Physical motivation for baryon femtoscopy
3. Existing data
4. Proposed measurements
5. Conclusions

# 1. Femtoscopy method

The observable of interest in femtoscopy is the two-particle correlation function, which is defined as the probability to find simultaneously two particles with momenta  $\mathbf{p}_1$  and  $\mathbf{p}_2$  divided by the product of the corresponding single particle probabilities

$$C(\mathbf{p}_1, \mathbf{p}_2) \equiv \frac{P(\mathbf{p}_1, \mathbf{p}_2)}{P(\mathbf{p}_1) \cdot P(\mathbf{p}_2)}. \quad (1)$$

These probabilities are directly related to the inclusive Lorentz invariant spectra  $P(\mathbf{p}_1, \mathbf{p}_2) = E_1 E_2 \frac{d^6 N}{d^3 p_1 d^3 p_2}$  and  $P(\mathbf{p}_{1,2}) = E_{1,2} \frac{d^3 N}{d^3 p_{1,2}}$ . In absence of a correlation signal the value of  $C(\mathbf{p}_1, \mathbf{p}_2)$  equals unity.

Eq. (1) can then be rewritten as  $C(\mathbf{k}^*) = \int d^3 r^* S(r^*) |\psi(r^*, \mathbf{k}^*)|^2$ , (2)

where  $k^*$  is the relative momentum of the pair defined as  $k^* = \frac{1}{2} \cdot |\mathbf{p}_1^* - \mathbf{p}_2^*|$ , with  $\mathbf{p}_1^*$  and  $\mathbf{p}_2^*$  the momenta of the two particles in the pair rest frame (PRF, denoted by the  $*$ ),  $S(r^*)$  contains the distribution of the relative distance of particle pairs in the pair rest frame, the so-called source function, and  $\psi(r^*, \mathbf{k}^*)$  denotes the relative wave function of the particle pair. The latter contains the particle interaction term

and determines the shape of the correlation function.

$$S(r_0, r) = 1 / (4\pi r_0^2)^{3/2} \exp(-r^2 / 4r_0^2)$$

where  $r_0$  is the size parameter of the source.

The complex scattering amplitude is evaluated by means of the effective range approximation

$$f_s(k^*) = 91 / f_{0_s} + d_{0_s} k^{*2} / 2 - i k^* \quad (-1)$$

with the scattering length  $f_{0_s}$ , the effective range  $d_{0_s}$  and  $s$  denoting the total spin of the particle pair.

R.Lednicky, V.L.Lyuboshitz, Sov.J.Nucl.Phys, 35, 770 (1982)

For review see M.A.Lisa et.al. Ann.Rev.Nucl.Part.Sci 55, 357 (2005)

10th Collaboration Meeting of the BM@N

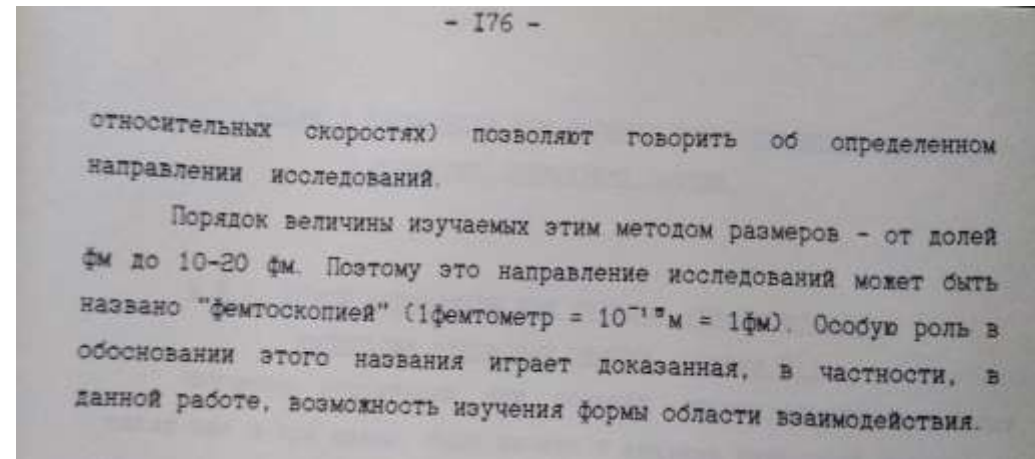
Experiment at NICA Facility, 14-19 May 2023

Traditionally femtoscopy is used to investigate the spatial-temporal evolution of the particle emitting source created during the collision. Assuming that the interaction for the employed particles is known, a detailed study of the geometrical extension of the emission region becomes possible.

In order to relate the correlation function to experimentally accessible quantities, Eq. (1) is reformulated [2] as

$$C(k^*) = \mathcal{N} \frac{A(k^*)}{B(k^*)}, \quad (3)$$

The distribution of particle pairs from the same event is denoted with  $A(k^*)$  and  $B(k^*)$  is a reference sample of uncorrelated pairs. The latter is obtained using event mixing techniques



А.С. Корреляции кумулятивных частиц, диссертация, 1991

# 1. Physical motivation for baryon femtoscopy

$$r_{p\Lambda} \leq r_{pn} \leq r_{pp} - \text{expectation}$$

A serious barrier to further progress in high energy physics is our lack of understanding of the process of hadronization, in which the quarks and gluons of perturbative QCD are converted into the hadrons that are seen in the detectors

## **String model of hadronization**

Strangeness and baryons enhancement in nucleus collisions – signal of a dense and hot QGP[1]?

One of the possible alternative - Lund strings hadronization model without QGP.

The strings close in space can fuse to form “color ropes” [2]. The increased energy density in a rope implies that more energy is released when a new quark-antiquark pair is produced (or a diquark-antidiquark pair in case of baryon production). This corresponds to a higher effective string tension  $k(k_{\text{eff}}) \sim 1 \text{ GeV/fm}$  during hadronization of a rope, which modifies the fragmentation parameters entering the Lund fragmentation function. Quark-antiquark production in a colour-electric field is regarded as a tunneling process[3], which gives a production probability for different quark flavours proportional to  $\exp(-\pi\mu^2/k)$

Such ropes are expected to give more strange particles and baryons[3].

[1] J.Rafelski and B.Muller, Phys.Rev.Lett.48(1982)1066

[2] T.S.Biro, H.B.Nielsen, and J.Knoll, Nucl.Phys. B245(1984) 449

[3] C.Bierlich, G.Gustafson, L.Lonnblad, and A.Tarasov, JHEP 03(2015)148

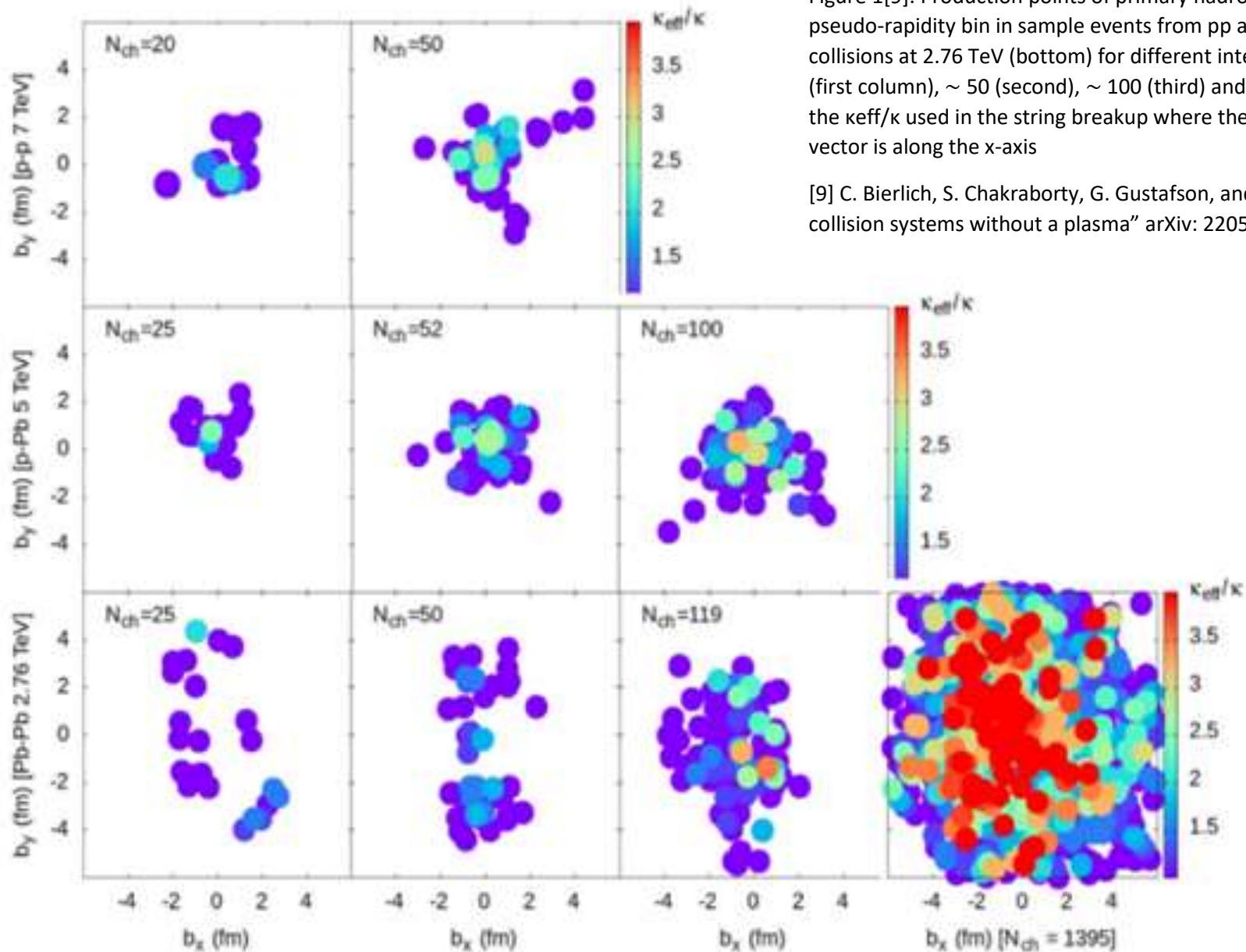


Figure 1[9]: Production points of primary hadrons in impact parameter space produced in the central pseudo-rapidity bin in sample events from pp at 7 TeV (top row), pPb at 5.02 TeV (middle), and PbPb collisions at 2.76 TeV (bottom) for different intervals of central ( $|\eta| < 0.5$ ) charged multiplicity:  $\sim 25$  (first column),  $\sim 50$  (second),  $\sim 100$  (third) and  $>1000$  (last column). The colour of the points indicates the  $\kappa_{\text{eff}}/\kappa$  used in the string breakup where the primary hadrons were produced. The impact parameter vector is along the x-axis

[9] C. Bierlich, S. Chakraborty, G. Gustafson, and L. Lönnblad, “Strangeness enhancement across collision systems without a plasma” arXiv: 2205.11170,[hep-ph],2022

### 3. Existing data(close to BM@N energy range)

## HADES, Phys.Rev.C82(2010)021901

$\Lambda p$

Ar+KCl, 1,756 AGeV, trigger:  $N_{ch} > 15$  for  $18^\circ < \theta < 85^\circ$   
(35% most central),  $0.7 \cdot 10^9$  events,  $\Lambda$ :  $m_\Lambda \pm 6$  MeV;  
 $2.4 \cdot 10^5$   $p\Lambda$  pairs, 1% -  $k < 0.1$  GeV, 0.1% (270 pairs) -  
 $k < 0.04$  GeV

Correlation function is defined as

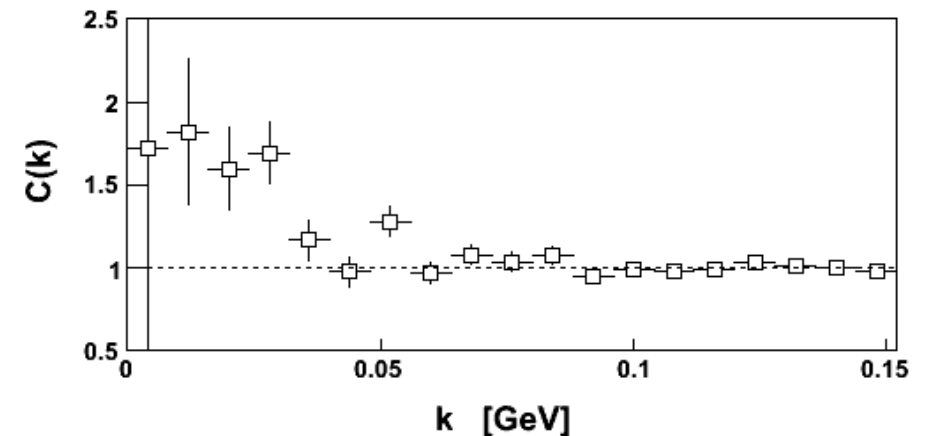
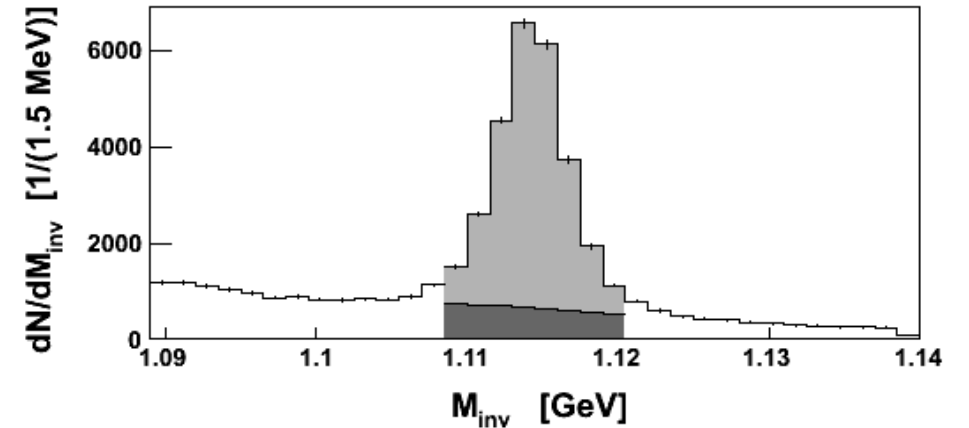
$$C(p_1, p_2) = Y_{12}(p_1, p_2) / Y_{12, \text{mix}}(p_1, p_2)$$

where  $Y_{12}$  - the coincidence yield of pairs of particles having the momenta  $p_1$  and  $p_2$  ;  
denominator - the same for mixed events.

Due to limited statistics the six-dimensional correlation function is projected onto one-half of the relative momentum in the pair c.m. frame  $\mathbf{k} = |\mathbf{p}_1 - \mathbf{p}_2|/2$ ,  
normalization:  $C(k) = 1$  for  $0.1 < k < 0.15$  GeV/c

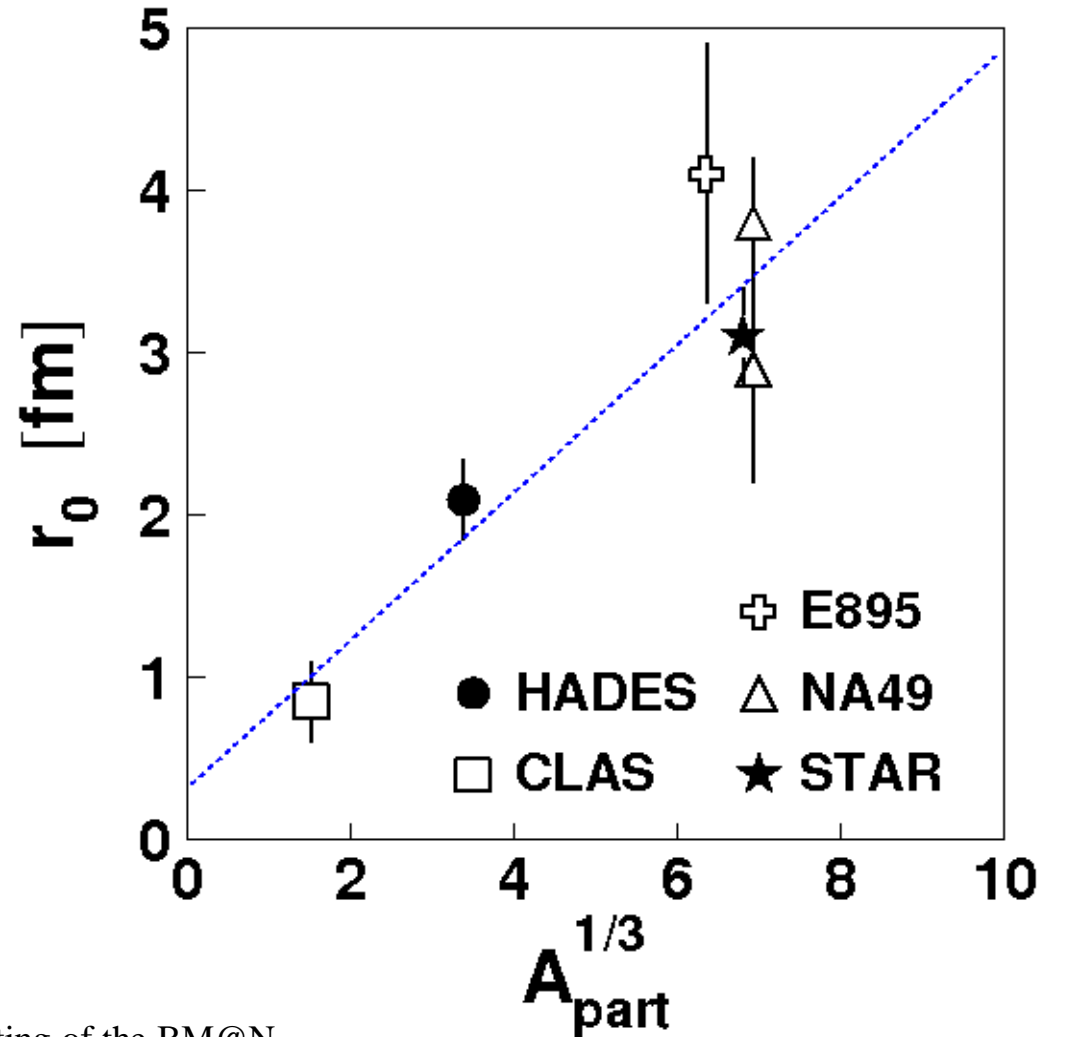
**Enhancement  $C(k)$  at small  $k$  -  
effect of the strong final state interaction (FSI)**

$r = 2.09 \pm 0.16$  fm (statistical error; 3 systematical errors each  $\sim 0.1$  fm due to close track correction, pair purity, and variation of the scattering lengths)



$\Lambda p$

- [3] P. Chung et al. (E895), Phys. Rev. Lett. 91, 162301 (2003).  
[4] C. Blume et al. (NA49), Nucl. Phys. A715, 55c (2003).  
[5] J. Adams et al. (STAR), Phys. Rev. C 74, 064906 (2005).  
[6] K.R. Mikhailov, A.V. Stavinsky, A.V. Vlassov, B.O. Kerbikov,  
and R. Lednicky (CLAS), Phys. Atom. Nucl. 72, 668 (2009);  
Acta Phys. Polon. B 40, 1171 (2009).



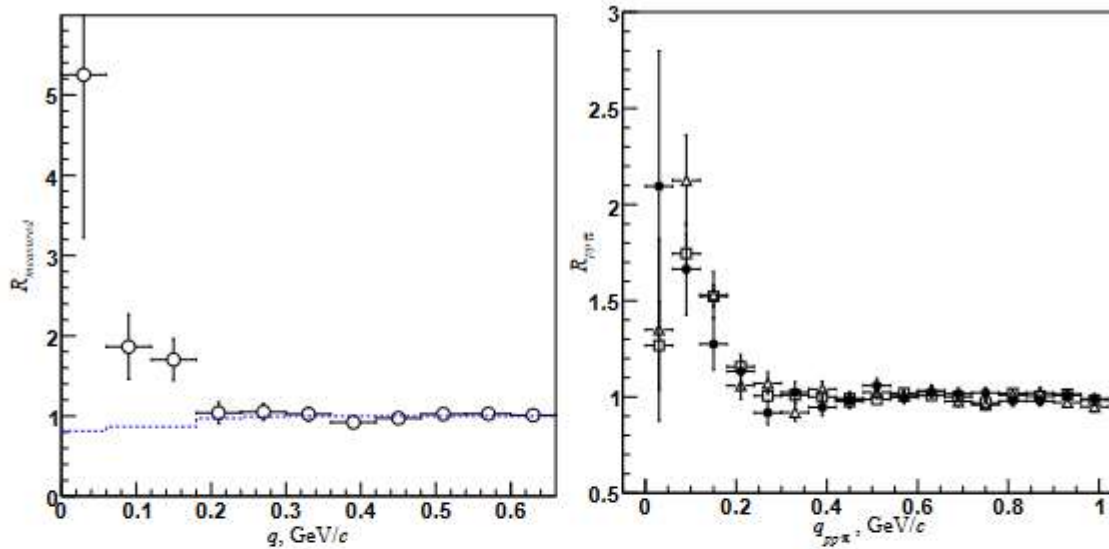
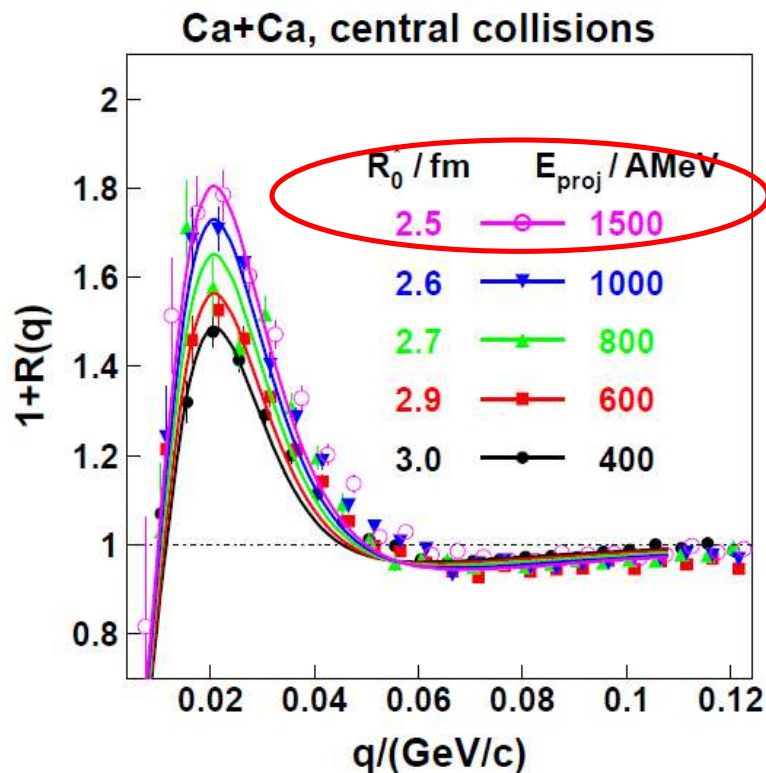


Fig. 2. Left: The measured  $p\Lambda$  correlation function *versus*  $q$ . The dashed line corresponds to the close-track efficiency correction for the measured  $p\Lambda$  correlation function. Right: Comparison of  $p$ - $p\pi$  correlation functions, which are measured by three different methods.

Since the  $\Lambda \rightarrow p\pi^-$  decay momentum (0.101 GeV/ $c$ ) is relatively small, one has to take into account the close-track efficiency for proton pairs [9] when the  $p\pi$ -pair mass is close to  $M_\Lambda$ . We apply close-track-efficiency correction for pair of protons in the same manner as in [2]. The close-track efficiency for measured correlation function is shown by the dashed line on Fig. 2 (left).

The  $p\Lambda$  correlation function is calculated according to the formula  $R_{p\Lambda,pp\pi} = \eta \cdot R_{p\Lambda} + (1 - \eta) \cdot R_{pp\pi}$ , where  $\eta \simeq 0.5$  is the ratio of  $\Lambda$  pairs to  $p\pi^-$  pairs when  $M_{p\pi} \sim M_\Lambda$ .  $R_{p\Lambda,pp\pi}$  is the measured correlation function, which is a combination of both  $p\Lambda$  and  $pp\pi$  correlation functions.

Phys.Atom.Nucl.72,668(2009)  
Acta Phys.Polon.B40,1171(2009)



## pp correlations

$\sigma_{\text{tof}} \sim 100 \text{ps}$ ,  $L \sim 400 \text{cm}$   
 $8.5^\circ < \theta < 26.5^\circ$ ;  
 Average imp. param.  $\sim 2\text{-}3 \text{fm}$   
 $A_{\text{part}} \sim 60 \text{(Ca)}, \sim 150 \text{(Ru)}, \sim 300 \text{(Au)}$   
 \*R.Kotte et al.(FOPI), Eur.Phys. J.A23,271(2005)

Fig. 5. Correlation functions of proton pairs from central collisions of Ca + Ca at projectile energies from 400 to 1500 A-MeV. Experimental data (symbols) are compared to predictions of the FSI model with Gaussian source and zero lifetime (lines). The corresponding apparent source radii are indicated.

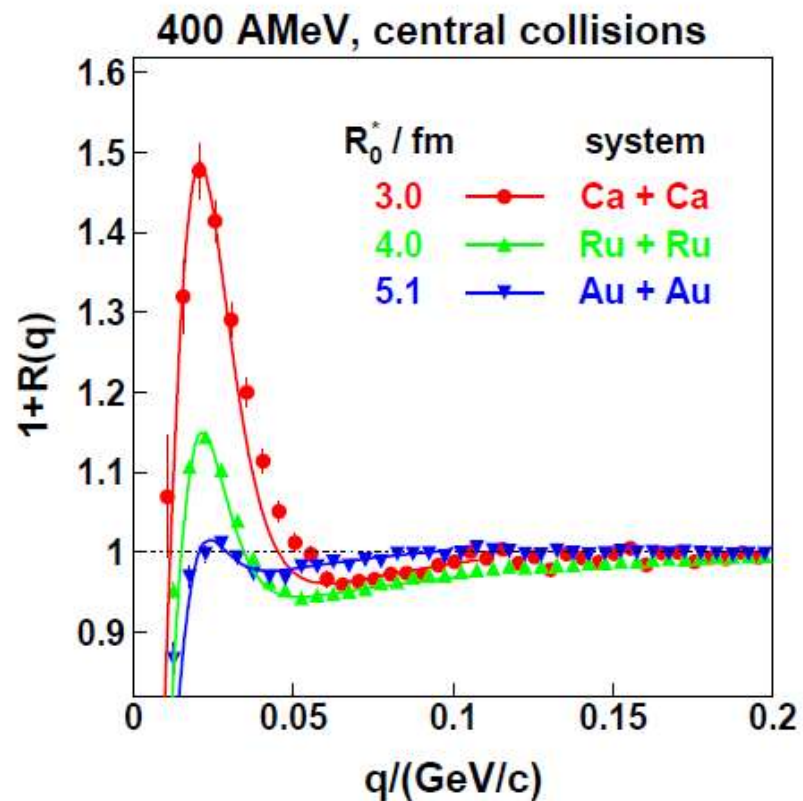


Fig. 1. Correlation functions of proton pairs from central collisions of Ca + Ca, Ru + Ru, and Au + Au at 400 A-MeV. Experimental data (symbols) are compared to predictions of the FSI model with Gaussian sources and zero lifetime (lines). The corresponding apparent source radii are indicated.

$R_0^* = (3.0 \pm 0.1) \text{ fm}$  for Ca + Ca,  $(4.0 \pm 0.15) \text{ fm}$  for Ru + Ru and  $(5.1 \pm 0.2) \text{ fm}$  for Au + Au collisions. Note

$r_{p\Lambda} \leq r_{pn} \leq r_{pp}$  - expectation

$r_{p\Lambda} < (?) r_{pp}$  - data

### **BM@N:**

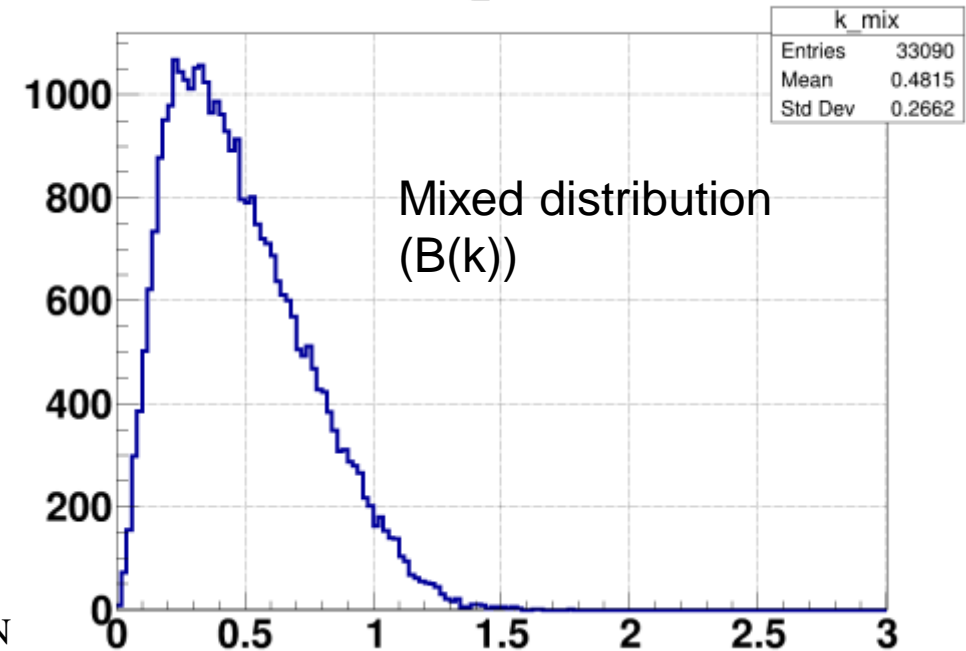
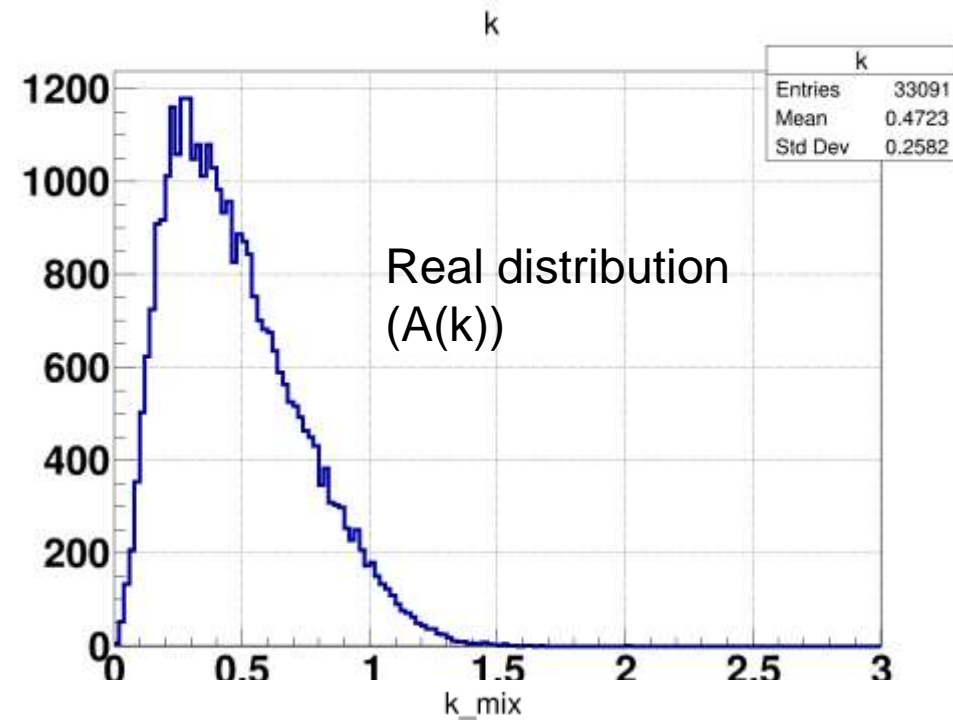
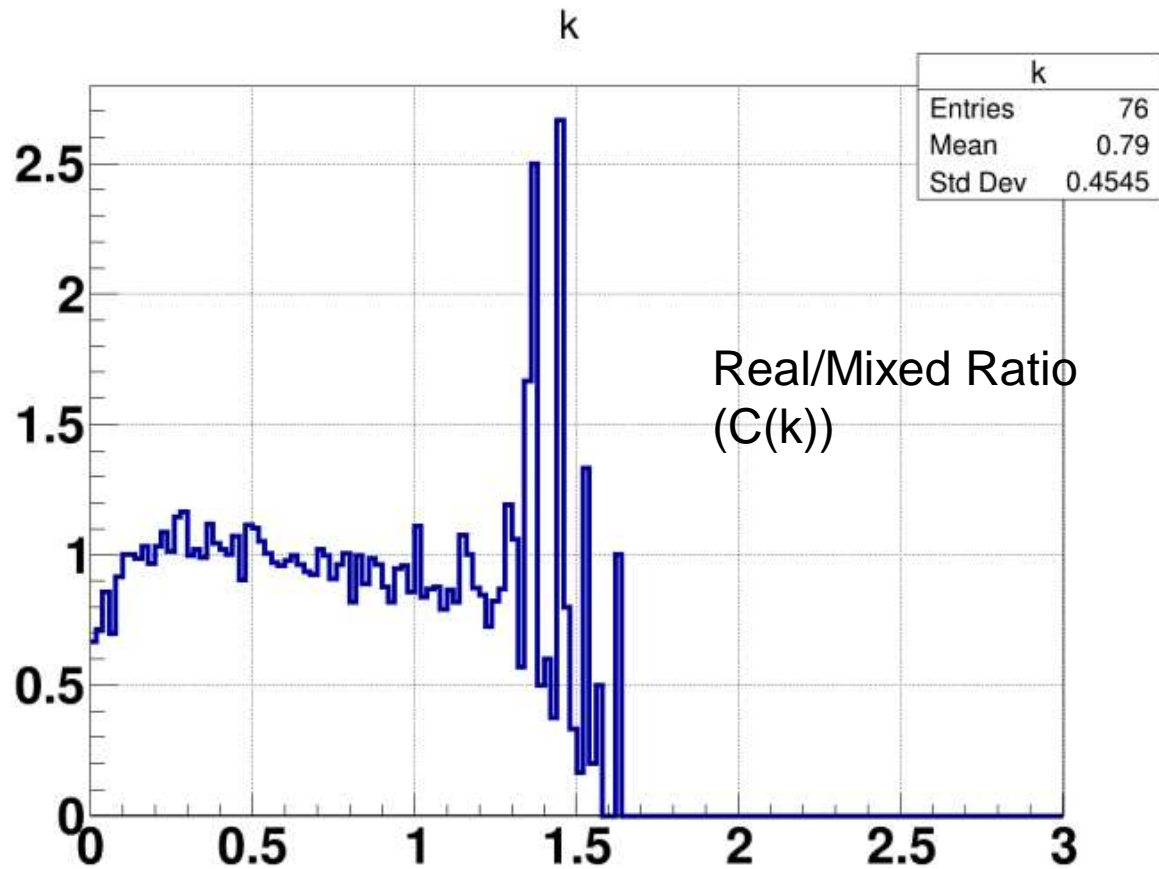
$r_{p\Lambda} < r_{pn} < r_{pp}$   
statistics, s/b ratio      HGN detector      Close track efficiency

## Close track efficiency

- 1) pd correlations (physics- $F(\delta p_{\text{pair-scm}}=2k)$ , efficiency- $f(\delta p_{\text{lab}})$ )
- 2) + forward detectors (**P.Alekseev report, this meeting**)

[BM@N](#) , pd correlations(**very preliminary**)

(Ar+C, Ar+Al, Ar+Cu, Ar+Sn, Ar+Pb at 3.2A GeV)



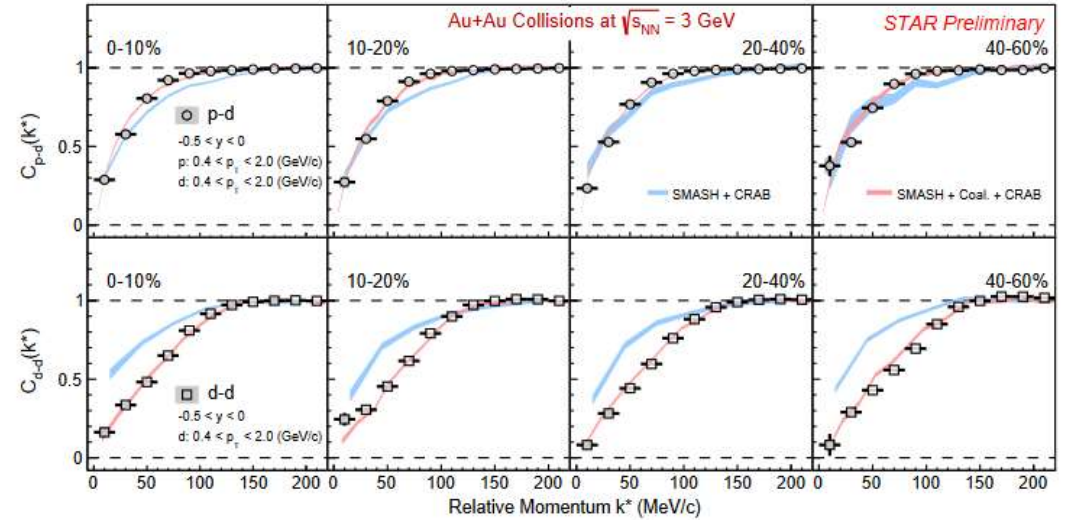
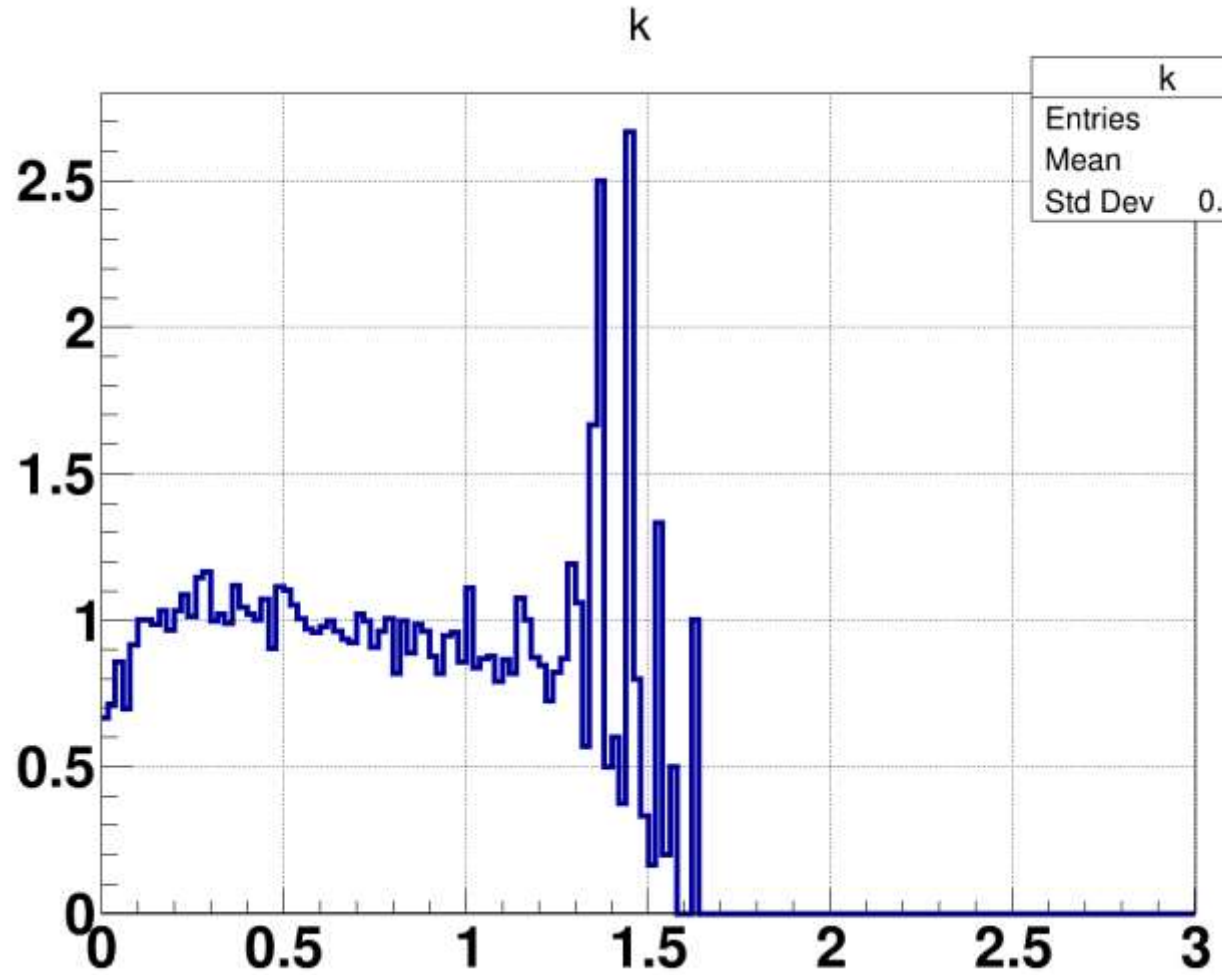
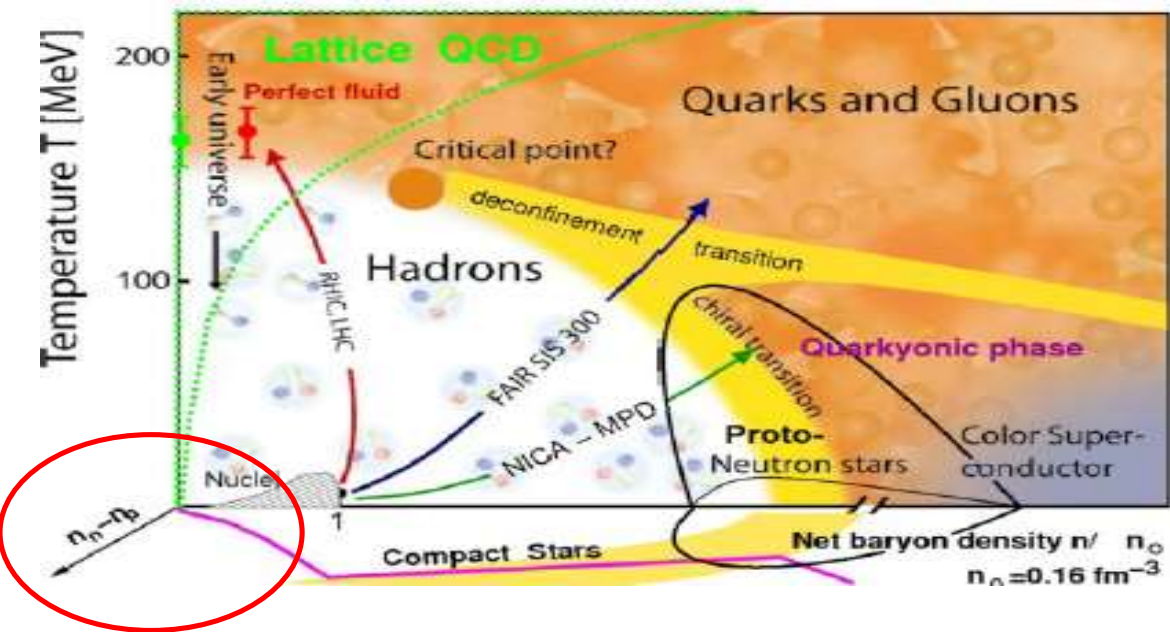


Fig. 4. The  $p-d$  and  $d-d$  correlation functions in different collision centralities in Au+Au collisions at  $\sqrt{s_{NN}} = 3$  GeV. The statistical and systematic errors are shown as vertical lines and grey bands, respectively. The colored bands represent the  $p-d$  and  $d-d$  correlations obtained with the deuteron from nucleon coalescence (red) in SMASH and directly produced from SMASH via hadronic scattering (blue), respectively.

STAR-(BES) ArXiv:2208.05722[nucl-ex],QM2022

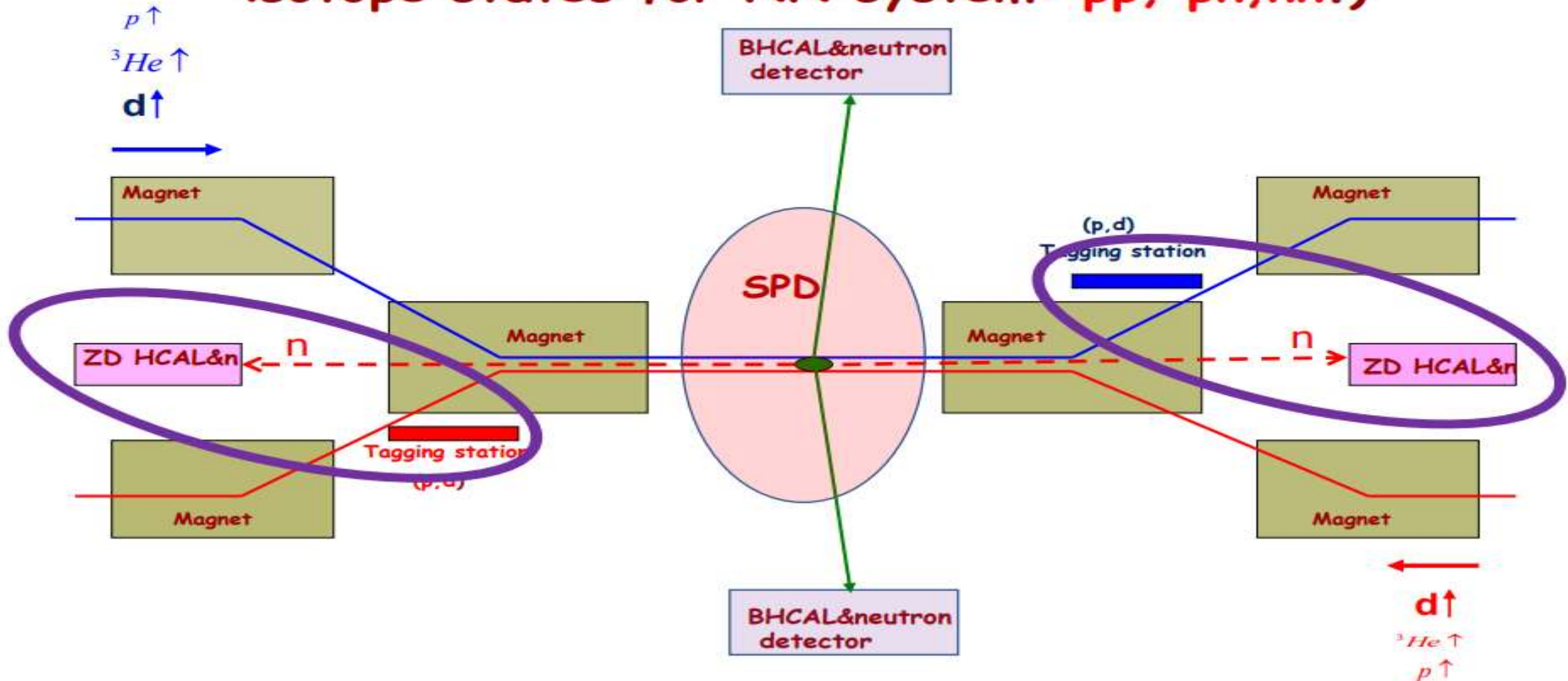
# Neutron detector. Motivation



1. Neutron is one of the main particle specie for AA collision at Nuclotron-NICA energy range;
2. State of nuclear matter depends on  $n/p$  ratio;
3. To identify some strange particles one need identify neutrons (for example  $\Sigma^+ \rightarrow n\pi^+$ );
4. Femtoscopy measurements: space time parameters for  $np$  and  $pp$ ,  $nn$  are different.

⇒ **Need to measure neutrons**

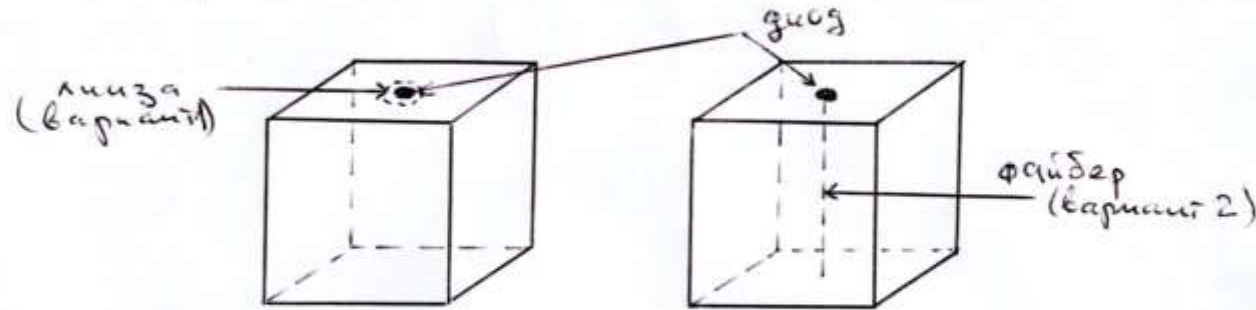
# NICA Collision place for SPIN physics (deuteron and other beams, the first time all isotope states for NN system: pp, pn, nn.)



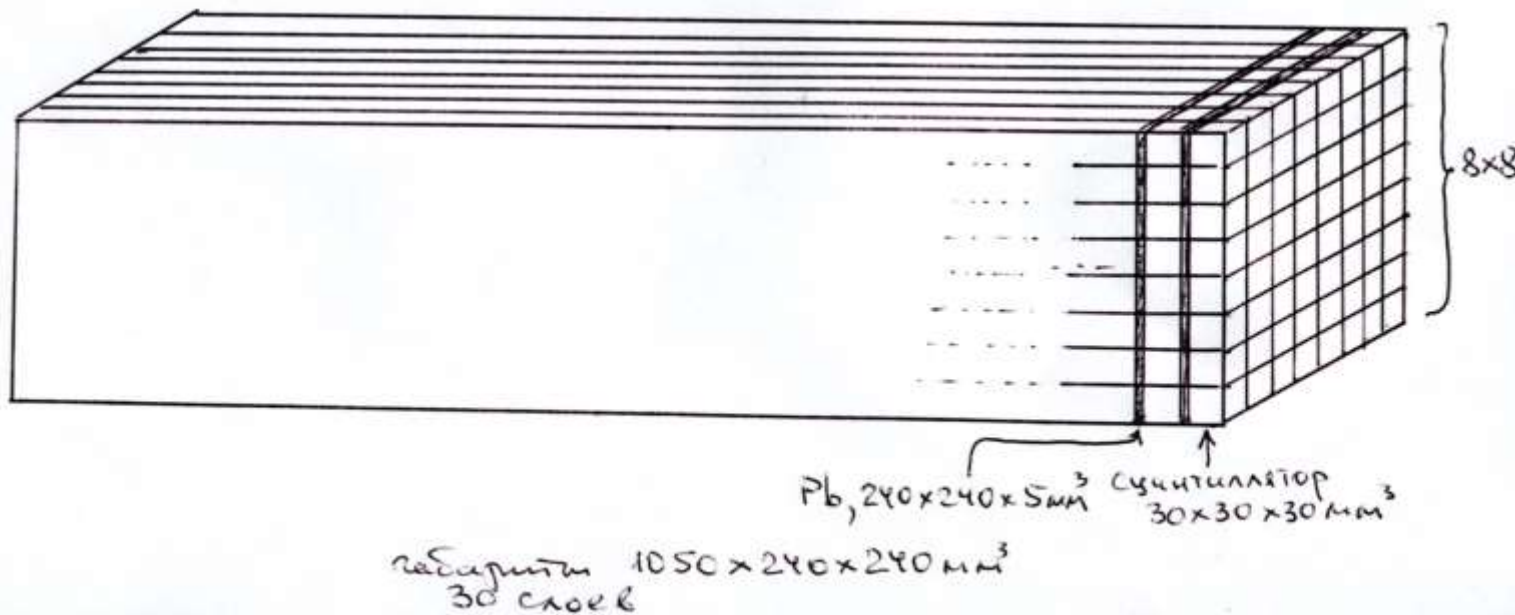
10th Collaboration Meeting of the BM@N  
Experiment at NICA Facility, 14-19 May 2023

**The tagging stations can be used as polarimeter!**

Стартовая конфигурация (7.2.2018, A.S.)



$64 \times 30 = 1920$  гнобов  
15 см Pb + 90 см сцинтиллятора (~1,5 + 1,1 эк. гл.)  
(~30 + 2 рас. гл.)



A.S., 2019, XII Черенковские чтения новые методы в экспериментальной ядерной физике и физике частиц; Зимняя школа ПИЯФ-ИТЭФ, 2019

BM@N HGN Propotype beam tests-  
D.Sakulin report, this meeting

## Conclusions

- 1) There are important femtoscopy tasks for [BM@N](#)
- 2)  $\Lambda p$  correlations can be studied with actual detector hard and soft configuration
- 3) feasibility for pp and np(with HGN detector) femtoscopy measurements have to be studied

Thanks for the attention!

Back up slides

If one considers smaller colliding systems such as proton-proton (pp) and assumes that the particle emitting source does not show a strong time dependence, **one can reverse the paradigm** and exploit femtoscopy to study the final state interaction (FSI).

Hyperon–nucleon and hyperon–hyperon interactions are still rather poorly experimentally constrained and a detailed knowledge of these interactions is necessary to understand quantitatively the strangeness sector in the low-energy regime of Quantum-Chromodynamics (QCD).

Hyperon–nucleon ( $p\text{-}\Lambda$  and  $p\text{-}\Sigma$ ) scattering experiments have been carried out in the sixties [1–3].

The measured cross sections have been used to extract scattering lengths and effective ranges for the strong nuclear potential by means of effective models such as the Extended-Soft-Core (ESC08) baryon–baryon model [4] or by means of chiral effective field theory ( $\chi$ EFT) approaches at leading order (LO) [5] and next-to-leading order (NLO) [6]. The results obtained from the above-mentioned models are rather different, but all confirm the attractiveness of the  $\Lambda$ –nucleon ( $\Lambda$ –N) interaction for low hyperon momenta. The existence of hypernuclei [7] confirms that the N– $\Lambda$  interaction is attractive within nuclear matter for densities below nuclear saturation  $\rho_0 = 0.16 \text{ fm}^{-3}$ .

[1] B. Sechi-Zorn, B. Kehoe, J. Twitty, and R. A. Burnstein, Phys. Rev. 175 (1968) 1735–1740. [2] F. Eisele, H. Filthuth, W. Foehlich, V. Hepp, and G. Zech, Phys. Lett. B37 (1971) 204–206. [3] G. Alexander et al., Phys. Rev. 173 (1968) 1452–1460. [4] M. M. Nagels, T. A. Rijken, and Y. Yamamoto, arXiv:1501.06636 [nucl-th]. [5] H. Polinder, J. Haidenbauer, and U.-G. Meißner, Nuclear Physics A 779 (2006) 244 – 266. [6] J. Haidenbauer, S. Petschauer, N. Kaiser, U. G. Meissner, A. Nogga, and W. Weise, Nucl. Phys. A915 (2013) 24–58, arXiv:1304.5339 [nucl-th]. [7] O. Hashimoto and H. Tamura, Prog. Part. Nucl. Phys. 57 (2006) 564–653.

Model	$f_0^{S=0}$ (fm)	$f_0^{S=1}$ (fm)	$d_0^{S=0}$ (fm)	$d_0^{S=1}$ (fm)	$n_\sigma$	
ND [77]	1.77	2.06	3.78	3.18	1.1	
NF [78]	2.18	1.93	3.19	3.358	1.1	
NSC89 [79]	2.73	1.48	2.87	3.04	0.9	
NSC97 [80]	a	0.71	2.18	5.86	2.76	1.0
	b	0.9	2.13	4.92	2.84	1.0
	c	1.2	2.08	4.11	2.92	1.0
	d	1.71	1.95	3.46	3.08	1.0
	e	2.1	1.86	3.19	3.19	1.1
	f	2.51	1.75	3.03	3.32	1.0
ESC08 [81]	2.7	1.65	2.97	3.63	0.9	
$\chi$ EFT	LO [25]	1.91	1.23	1.4	2.13	1.8
	NLO [26]	2.91	1.54	2.78	2.72	1.5
Jülich	A [82]	1.56	1.59	1.43	3.16	1.0
	J04 [83]	2.56	1.66	2.75	2.93	1.4
	J04c [83]	2.66	1.57	2.67	3.08	1.1

**Table 4:** Scattering parameters for the  $p$ - $\Lambda$  system from various theoretical calculations [25, 26, 77–83] and the corresponding degree of consistency with the experimentally determined correlation function expressed in numbers of standard deviations  $n_\sigma$ . The  $\chi$ EFT scattering parameters are obtained at a cutoff scale  $\Lambda = 600$  MeV. The usual sign convention of femtoscopy is employed where an attractive interaction leads to a positive scattering length.

[25] H. Polinder, et al., J. Nuclear Physics A 779 (2006) 244 – 266.

[26] J. Haidenbauer, et al., Nucl. Phys. A915 (2013) 24–58.

[77] M. M. Nagels, et al., Phys. Rev. D 15 (May, 1977) 2547

[78] M. M. Nagels, et al., Phys. Rev. D 20 (Oct, 1979) 1633

[79] P. M. M. Maessen, et al., Phys. Rev. C 40 (Nov, 1989) 2226

[80] T. A. Rijken, et al., Phys. Rev. C 59 (Jan, 1999) 21

[81] T. A. Rijken, et al., Progr.Theor. Phys.Suppl. 185 (2010) 14

[82] B. Holzenkamp, et al., Nucl. Phys. A 500 no. 3, (1989) 485

[83] J. Haidenbauer and U.-G. Meißner, Phys. Rev. C 72 (Oct, 2005) 044005 Meeting of the BM@N

Experiment at NICA Facility, 14-19 May 2023

The Table from: ALICE,  
Phys.Rev.C99(2019)2,024001,e-  
print-1805.12455[nucl-ex]

$f_0(S=0) \sim 2.0$ fm,  $f_0(S=1) \sim 1.8$ fm  
– the difference between model  
predictions is not so large

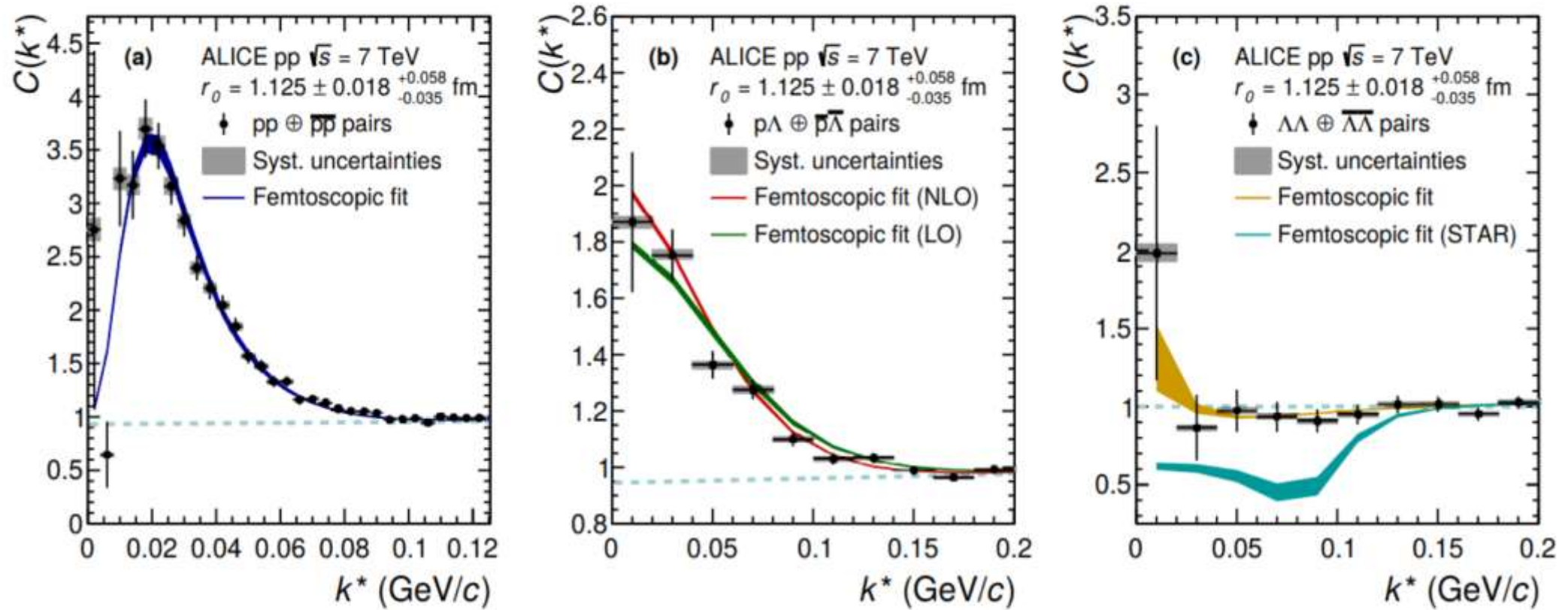


**Fig. 3:** (Color online) The p–p (a), p– $\Lambda$  (b) and  $\Lambda$ – $\Lambda$  (c) correlation function with a simultaneous fit with the NLO expansion (red line) for the scattering parameter of p– $\Lambda$  [26]. The dashed line denotes the linear baseline. After the fit is performed the LO [25] parameter set (green curve) is plugged in for the p– $\Lambda$  system and the scattering length obtained from [16] for the  $\Lambda$ – $\Lambda$  system (cyan curve).

ALICE, Phys.Rev.C99(2019)2,024001-e-Print:1805.12455[nucl-ex]

The situation for the  $\Sigma$  hyperon is currently rather unclear. There are some experimental indications for the formation of  $\Sigma$ -hypernuclei [28, 29] but different theoretical approaches predict both attractive and repulsive interactions depending on the isospin state and partial wave [24, 26, 30]. The scarce experimental data for this hypernucleus prevents any validation of the models. A  $\Xi$ -hypernucleus candidate was detected [31] and ongoing measurements suggest that the  $N$ - $\Xi$  interaction is weakly attractive [32]. A recent work by the Lattice HAL-QCD Collaboration [33] shows how this attractive interaction could be visible in the  $p$ - $\Xi$  femtoscopy analysis, in particular by comparing correlation functions for different static source sizes. This further motivates the extension of the femtoscopic studies from heavy ions to  $pp$  collisions since in the latter case the source size decreases by about a factor of three at the LHC energies leading to an increase in the strength of the correlation signal [34]. If one considers hyperon-hyperon interactions, the most prominent example is the  $\Lambda$ - $\Lambda$  case. The Hdibaryon  $\Lambda$ - $\Lambda$  bound state was predicted [35] and later a double  $\Lambda$  hypernucleus was observed [36]. From this single measurement a shallow  $\Lambda$ - $\Lambda$  binding energy of few MeV was extracted, but the Hdibaryon state was never observed. Also recent lattice calculations [37] obtain a rather shallow attraction for the  $\Lambda$ - $\Lambda$  state

The femtoscopy technique was employed by the STAR collaboration to study  $\Lambda$ - $\Lambda$  correlations in Au–Au collisions at  $\sqrt{s_{NN}} = 200$  GeV [16]. First a shallow repulsive interaction was reported for the  $\Lambda$ - $\Lambda$  system, but in an alternative analysis, where the residual correlations were treated more accurately [38], a shallow attractive interaction was confirmed. These analyses demonstrate the limitations of such measurements in heavy-ion collisions, where the source parameters are time-dependent and the emission time might not be the same for all hadron species.

The need for more experimental data to study the hyperon–nucleon, hyperon–hyperon and even the hyperon–nucleon–nucleon interaction has become more crucial in recent years due to its connection to the modeling of astrophysical objects like neutron stars [39–42]. In the inner core of these objects the appearance of hyperons is a possible scenario since their creation at finite density becomes energetically favored in comparison with a purely neutron matter composition [41]. However, the appearance of these additional degrees of freedom leads to a softening of the nuclear matter equation of state (EOS) [43] making the EOS incompatible with the observation of neutron stars as heavy as two solar masses [44, 45]. This goes under the name of the ‘hyperon puzzle’. Many attempts were made to solve this puzzle, e.g. by introducing three-body forces for  $\Lambda$ NN leading to an additional repulsion that can counterbalance the large gravitational pressure and finally allow for larger neutron star masses [46–49]. A repulsive core for the two body forces would also stiffen the EOS containing hyperons. In order to constrain the parameter space of such models a detailed knowledge of the hyperon–nucleon, including  $\Sigma$  and  $\Xi$  states, and of the hyperon–nucleon–nucleon interaction is mandatory

# Cluster model of hadronization

1. **Parton shower**
2. **Split the gluons** left at the end of the parton shower **into (di)quark-anti(di)quark pairs**. The gluon is allowed to decay isotropically into any of the accessible quark flavours with probability given by the available phase space for the decay
3. Initial **cluster formation**. Colour singlets pairs of partons((di)quarks and anti-(di)quarks) are formed into clusters with the the momentum given by the sum of the momenta of the constituent partons
4. The **clusters** can be regarded as highly excited hadron resonances ( $M \sim 0.5-3\text{GeV}$ ) and **decayed**, according to phase space, **into pair of observed hadrons**. There is however a small fraction of clusters that are too heavy for this to be reasonable approach. These heavy clusters are therefore first split into lighter clusters before they decay. A cluster is split into two clusters if the mass,  $M <$  is such that  $M^{C_{\text{low}}} > C_{\text{max}}^{C_{\text{low}}} + (m_1 + m_2)^{C_{\text{low}}}$ , where  $C_{\text{max}}$  and  $C_{\text{low}}$  are parameters of the model,  $m_{1,2}$  are the masses of the constituent partons of the cluster

M.Bahr et al., arXiv:0803.0883[hep-ph]2008